



In situ studies of the oxidation of HCl over RuO₂ model catalysts: Stability and reactivity

S. Zweidinger^a, J.P. Hofmann^a, O. Balmes^b, E. Lundgren^c, H. Over^{a,*}

^a Department of Physical Chemistry, Justus-Liebig-University, Heinrich-Buff-Ring 58, D-35392 Gießen, Germany

^b Beamline ID03, European Synchrotron Radiation Facility (ESRF), BP 220, F-38043 Grenoble Cedex 9, France

^c Department of Synchrotron Radiation Research, Lund University, Sölvegatan 14, S-22362 Lund, Sweden

ARTICLE INFO

Article history:

Received 21 January 2010

Revised 23 February 2010

Accepted 25 February 2010

Available online 31 March 2010

Keywords:

Heterogeneous catalysis

Surfaces

Deacon process

In situ SXRD

Stability

Reactivity

RuO₂

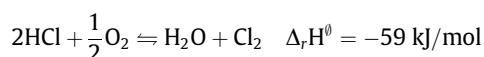
ABSTRACT

Structure–activity experiments were performed for the HCl oxidation reaction (Deacon-like process) over RuO₂ model catalysts – RuO₂(1 1 0) and RuO₂(1 0 0) – applying in situ surface X-ray diffraction (SXRD) combined with on-line mass spectrometry. The studied model catalysts turned out to be long-term stable under reaction conditions with gas feed ratios p(HCl):p(O₂) ranging from 1:4 to 4:1 in the mbar pressure regime and temperatures as high as 685 K. Even pure HCl exposure in the mbar regime was not able to reduce RuO₂ below 600 K; above 650 K chemical reduction of the oxide sets in. Under strongly oxidizing reaction conditions, the (surface) oxides grow slowly in thickness. On-line reactivity experiments of both types of model catalysts in a batch reactor yield a mean turn-over frequency (TOF) of 0.6 Cl₂ molecules per second and active site for the HCl oxidation at 650 K and initial partial pressures of p(HCl) = 2 mbar and p(O₂) = 0.5 mbar. The HCl oxidation over RuO₂ is therefore considered to be structure insensitive.

© 2010 Elsevier Inc. All rights reserved.

1. Introduction

The heterogeneously catalyzed HCl oxidation (so-called Deacon process)



is an ideal way to chemically transform HCl back to Cl₂, allowing for the design of energy-efficient closed process cycles in industrial (chlorine-related) chemistry. Although the Deacon process has been around for some 140 years [1], it had not found its way into commercial applications. The reasons are manifold, but the original Deacon process catalyzed by CuO/CuCl₂ has suffered most notably from the missing stability of the deployed catalyst and from reaction temperatures above 700 K, which results in a low turnover for thermodynamic reasons. Note that the oxidation of HCl is only mildly exothermic by –59 kJ/mol (Cl₂) so that the final yield at 700 K is given by the equilibrium conversion of only 70–80%. Over the past 140 years, numerous strategies have been pursued to overcome the problems with the original Deacon process, although with only limited success [2–7]. Therefore, the Deacon process was even-

tually abandoned and displaced by electrolysis, a prohibitively energy consuming process [8].

Only recently Sumitomo Chemical [9] discovered an efficient and stable Deacon-like process on the basis of RuO₂-covered TiO₂ (referred to as Sumitomo process). The Sumitomo process is a true breakthrough in recent catalysis research since chlorine can now be recycled from HCl with low energy cost and high conversion yields of 95%. The unit energy consumption of the Sumitomo process is only 15% of that required by the recently developed Bayer and UhdeNora electrolysis method [8]. In retrospect RuO₂-based catalysts seem to be the obvious choice for the Deacon process since such catalysts have already been in industrial use as dimensionally stable anodes (DSA) in the chlorine-alkali electrolysis for more than 40 years [10]. However, this hindsight reveals a quite general problem of a highly specialized scientific society in that the expertise of even closely related chemical disciplines such as electro catalysis and heterogeneous catalysis is distributed and well separated in two non-interacting scientific communities. Modern catalysis research needs to overcome this community gap for future innovations [11,12].

In recent publications, the extraordinary stability of RuO₂ in the Sumitomo process has shown to be attributed to the replacement of bridging oxygen (O_{br}, cf. Fig. 1) by chlorine, a process which is confined only to the top-most layer of RuO₂(1 1 0) [13]. A deeper reduction/chlorination of the oxide has not been observed under ultra high vacuum (UHV)-typical conditions. The mechanism of

* Corresponding author. Fax: +49 641 9934559.

E-mail address: Herbert.Over@phys.chemie.uni-giessen.de (H. Over).

URL: <http://www.uni-giessen.de/cms/physchem/over> (H. Over).

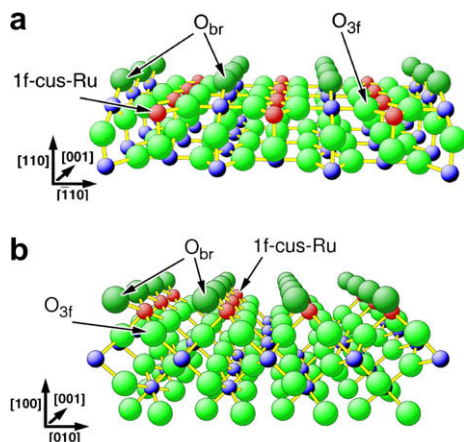


Fig. 1. Ball and stick model of the $\text{RuO}_2(1\ 1\ 0)$ (a) and the $\text{RuO}_2(1\ 0\ 0)$ (b) surfaces. Large (green) balls represent oxygen and small (red, blue) balls ruthenium atoms of $\text{RuO}_2(1\ 1\ 0)$ and $\text{RuO}_2(1\ 0\ 0)$. The under coordinated surface sites, namely the bridge-bonded O species (O_{br}) and the onefold under coordinated Ru (1f-cus Ru) are indicated. (For interpretation of the references to color in this figure legend, the reader is referred to the web version of this article.)

the oxidation of HCl with oxygen producing Cl_2 and water has been identified with a one-dimensional Langmuir–Hinshelwood (LH) mechanism along the rows of under coordinated Ru sites (1f-cus Ru) on the chlorine-stabilized $\text{RuO}_2(1\ 1\ 0)$ surface [14]; similar results about the reaction mechanism were published by Lopez et al. for powder RuO_2 [15]. Oxydehydrogenation of adsorbed HCl by on-top oxygen produces Cl adsorbed on-top of 1f-cus Ru. The recombination of two such neighboring Cl_{or} atoms to form Cl_2 constitutes the rate-determining step [14,15], an elementary reaction step which is activated by 115 kJ/mol. All these conclusions about the reaction mechanism and the stability of the $\text{RuO}_2(1\ 1\ 0)$ model catalyst are drawn from experiments performed under UHV-conditions, i.e. pressures below 10^{-6} mbar. However, it is known that catalytic performance may change dramatically with increasing pressure, thereby opening a so-called pressure gap [16].

In this paper, we report on combined stability and activity experiments of two model catalysts $\text{RuO}_2(1\ 1\ 0)$ and $\text{RuO}_2(1\ 0\ 0)$ under HCl oxidation conditions up to a pressure of 4 mbar and sample temperatures up to 685 K. While these pressures are not equivalent to those used in the industrial Deacon process (1–10 bar), the present measurements in the mbar range provide a useful link between UHV measurements and real catalytic conditions. The $\text{RuO}_2(1\ 1\ 0)$ and $\text{RuO}_2(1\ 0\ 0)$ surfaces turned out to be long-term stable over 15 h under such harsh reaction conditions as monitored by in situ SXRDX measurements. Even in a pure HCl atmosphere of 2 mbar, the oxide surface is stable up to 600 K, while beyond 650 K chemical reduction sets in. For the case of 2 mbar of HCl and 0.5 mbar of O_2 and a reaction temperature of 650 K, we determined a mean turn-over frequency (TOF) of 0.6 Cl_2 molecules per active catalyst site and second, independent of the two investigated surface orientations. Therefore, the HCl oxidation reaction is presumed to be not structure sensitive.

2. Experimental details

For the in situ SXRDX diffraction experiments, a new chamber was designed with a cylindrical X-ray window made from 1-mm thick aluminum instead of commonly used beryllium [17]. This modification of an existing chamber was required because extensive HCl exposure would have made the Be window brittle. With the unique high-pressure chamber of ID03 at ESRF [18], we were able to follow both the surface structure of the Ru-based model

catalyst by SXRDX and the reaction progress via on-line mass spectrometry (MS) during the HCl oxidation reaction over $\text{RuO}_2(1\ 1\ 0)$ and $\text{RuO}_2(1\ 0\ 0)$ model catalysts under nearly practical reaction conditions. The sample was mounted on a BN-encapsulated heater, and the temperature was measured by a Re/W (W5) thermocouple on the heater plate. In the reaction experiments, the high-pressure cell with a volume of about $2\ \text{dm}^3$ served as a batch reactor. The chamber could be separated from the pumping system by a gate valve. Since HCl and Cl_2 deteriorate significantly the sensitivity of the mass spectrometer (MS) with time, we only took an assay of the reaction mixture every 2 h by leaking the gas mixture from the batch reactor into the differentially pumped MS chamber for 30 min (pressure in MS chamber during the duty cycle: 3×10^{-6} mbar). With the present MS, we were not sensitive enough to detect Cl_2 , and the actual HCl partial pressure in the reaction chamber was affected by condensation at the chamber walls. Therefore, we followed the reaction progress with the decline in the O_2 partial pressure (MS) signal as a function of reaction time. The reaction mixture contained 1 or 2 mbar of Ar in order to calibrate the oxygen mass spectrometer signal against a constant Ar signal, thereby compensating for the HCl- and Cl_2 -induced sensitivity loss of the MS. For the SXRDX experiments, a photon energy of 20 keV was selected with a Si(1 1 1) monolithic channel cut monochromator corresponding to a wave length of 0.620 Å. The high photon energy is necessary for the Al-windows to achieve high transmission. The present paper focuses mainly on the actual structural status of the RuO_2 -based model catalysts – $\text{RuO}_2(1\ 1\ 0)$ and $\text{RuO}_2(1\ 0\ 0)$ – during the HCl oxidation reaction in the mbar range and temperatures up to 685 K addressing the following questions: How stable is the oxide and which structural parameters change during the reaction? Activity data are merely taken to complement these structural studies, since extended reactivity experiments are incompatible with the strict time constraints imposed by a beamtime at ESRF.

The particular surface orientations of RuO_2 were chosen because of their low surface energies rendering them the most prevailing facets in RuO_2 powder catalysts [13]. A second reason is that both orientations can be easily prepared on single crystal Ru surfaces, namely $\text{Ru}(0\ 0\ 0\ 1)$ and $\text{Ru}(1\ 0\ \bar{1}\ 0)$. The ultra thin RuO_2 films on $\text{Ru}(0\ 0\ 0\ 1)$ and $\text{Ru}(1\ 0\ \bar{1}\ 0)$ were always produced prior to the actual HCl oxidation experiment by exposing the metallic surface to 10^{-3} mbar of O_2 at 680 K for 20 min [19,20]. The resulting ultra thin $\text{RuO}_2(1\ 1\ 0)$ film with an averaged thickness of 2.5 nm fully covered the $\text{Ru}(0\ 0\ 0\ 1)$ surface, while the ultra thin $\text{RuO}_2(1\ 0\ 0)$ film fully covered the $\text{Ru}(1\ 0\ \bar{1}\ 0)$ surface with an averaged thickness of 3.8 nm.

In the bulk structure of RuO_2 , the Ru atoms bind to six oxygen atoms, forming a slightly distorted RuO_6 octahedron. The O atoms are coordinated to three Ru atoms in a planar sp^2 configuration. On the stoichiometric $\text{RuO}_2(1\ 1\ 0)$ surface (cf. the ball and stick model of the bulk-truncated $\text{RuO}_2(1\ 1\ 0)$ surface: Fig. 1a), two kinds of under coordinated surface atoms are present: (i) the bridging oxygen atoms O_{br} , which are coordinated only to two Ru atoms underneath (instead of three) and (ii) the so-called 1f-cus Ru atoms (1f-cus stands for onefold coordinatively unsaturated sites) [21], which are coordinated to five instead of six O atoms. The $\text{RuO}_2(1\ 0\ 0)$ surface exposes bridging O atoms and 1f-cus Ru atoms as well. The major difference between the two surface orientations is illustrated in Fig. 1. On $\text{RuO}_2(1\ 0\ 0)$ (cf. Fig. 1b), the bridging O atoms and the 1f-cus Ru atoms are attached to each other, while on $\text{RuO}_2(1\ 1\ 0)$ (cf. Fig. 1a), both kinds of under coordinated surface atoms are well separated. This structural difference may affect both the activity and stability during the catalytic HCl oxidation reaction over RuO_2 .

In reciprocal space, \mathbf{H} and \mathbf{K} are the in-plane lattice vectors corresponding to the in-plane lattice vectors \mathbf{a}_1 and \mathbf{a}_2 of the

Ru(0001) surface (with a length of 2.71 Å), and \mathbf{L} is the reciprocal out-of-plane vector corresponding to \mathbf{a}_3 (with a length of 4.28 Å). The reciprocal lattice vectors \mathbf{h} , \mathbf{k} , and \mathbf{l} of the epitaxially grown tetragonal RuO₂(110) (in-plane lattice constants: 3.11 Å and 6.28 Å) on Ru(0001) are given in fractions of \mathbf{H} , $\mathbf{H} + \mathbf{K}$ and \mathbf{L} (cf. Fig. 2a), respectively.

Similarly, the in-plane reciprocal lattice vectors of the Ru(10 $\bar{1}$ 0), \mathbf{H} and \mathbf{K} are given by their in-plane lattice vectors \mathbf{a}_1 and \mathbf{a}_2 with lengths of 2.71 Å and 4.28 Å, respectively. \mathbf{L} is the reciprocal out-of-plane vector corresponding to \mathbf{a}_3 (with a length of 4.69 Å). The reciprocal lattice vectors \mathbf{h} , \mathbf{k} , and \mathbf{l} of the tetragonal RuO₂(100) (in-plane lattice constants: 3.08 Å and 4.28 Å) on Ru(10 $\bar{1}$ 0) are also given in fractions of \mathbf{H} , \mathbf{K} and \mathbf{L} (cf. Fig. 2b). Note that a value of 3.08 Å is slightly smaller than the bulk-truncated parameter of 3.11 Å. In order to illustrate where peak intensities from the oxide surface are expected in reciprocal space, we show in Fig. 2 typical h-scans of RuO₂(110)/Ru(0001) and RuO₂(100)/Ru(10 $\bar{1}$ 0). Clearly, on Ru(0001) at $h = 0.73$ ($k = 0$, $l = 1.3$), a RuO₂(110)-related diffraction peak is discernible, while on Ru(10 $\bar{1}$ 0) at $h = 0.88$ ($k = 0$, $l = 1.02$), a strong RuO₂(100)-derived diffraction feature occurs.

3. Results and discussion

In the structure/activity experiments presented in this paper, we always start with a freshly oxidized surface of Ru(0001) or

Ru(10 $\bar{1}$ 0) depending on which orientation of the RuO₂ oxide surface we are focusing on. The temperature-dependent diffraction data were corrected for by the Debye–Waller factor.

3.1. Stability experiments in pure HCl atmosphere

We studied first the stability of RuO₂(110) against pure HCl, the most reducing condition which the model catalysts can encounter in the HCl oxidation reaction. We started from an oxidized RuO₂(110) surface with a layer thickness of 2.6 nm, admitted 1 mbar of pure HCl to the reaction chamber (batch reactor) and subsequently, increased the sample temperature stepwise from 300 K to 685 K.

Below a sample temperature of 600 K, the surface is stable (cf. Fig. 3) in that neither the oxide thickness (as derived from the full width at half maximum (FWHM) of the oxide-related peak in the l-scans: not shown) nor the surface area of the oxide did change (as determined by the FWHM of the oxide-related peak in the h-scans). Only above 650 K, the oxide disappeared rapidly as indicated by the intensity drop of the (0.73, 0, 1.3) beam. On first sight, this experimental finding is quite puzzling since hydrogen and methanol (MeOH) exposure readily reduce the RuO₂(110) surface beyond 400 K [22,23]. The reduction process of RuO₂(110) with hydrogen and MeOH is self-poisoned by the produced water so that the sample temperature has to be at least 400 K in order to liberate the water from the surface. With HCl exposure, the required

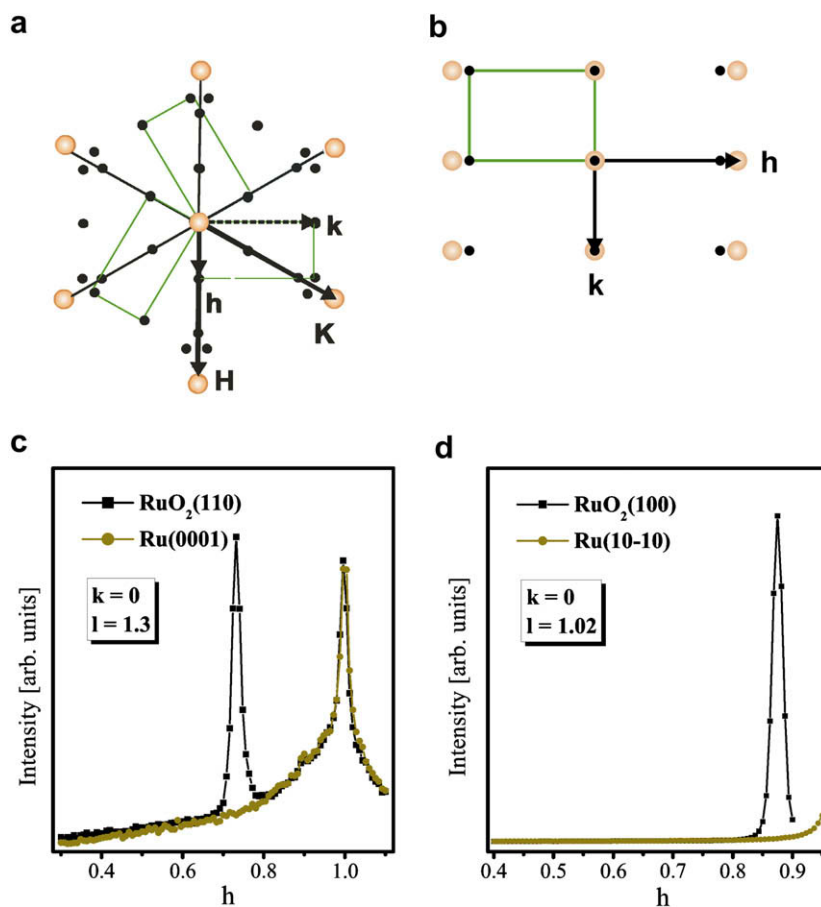


Fig. 2. (a) Schematic in-plane diffraction pattern of Ru(0001) (large shadowed disks) and RuO₂(110) (small black disks). In reciprocal space, the in-plane high-symmetry directions are denoted by \mathbf{H} and \mathbf{K} for Ru(0001). The reciprocal lattice vectors \mathbf{h} , \mathbf{k} of RuO₂(110) are given in fractions of \mathbf{H} and $\mathbf{H} + \mathbf{K}$. (b) Schematic in-plane diffraction pattern of Ru(10 $\bar{1}$ 0) (open disks) and RuO₂(100) (small solid disks). In reciprocal space, the in-plane high-symmetry directions are denoted by \mathbf{H} , \mathbf{K} for Ru(10 $\bar{1}$ 0). The reciprocal lattice vectors \mathbf{h} , \mathbf{k} of RuO₂(100) are given in fractions of \mathbf{H} and \mathbf{K} . (c) Typical h-scans for Ru(0001) in comparison with RuO₂(110)-covered Ru(0001) surface. The oxide peak appears at $h = 0.73$, while keeping $k = 0$, $l = 1.3$. (d) Typical h-scans for Ru(10 $\bar{1}$ 0) in comparison with RuO₂(100)-covered Ru(10 $\bar{1}$ 0) surface. The oxide peak appears at $h = 0.88$, while keeping $k = 0$, $l = 1.02$.

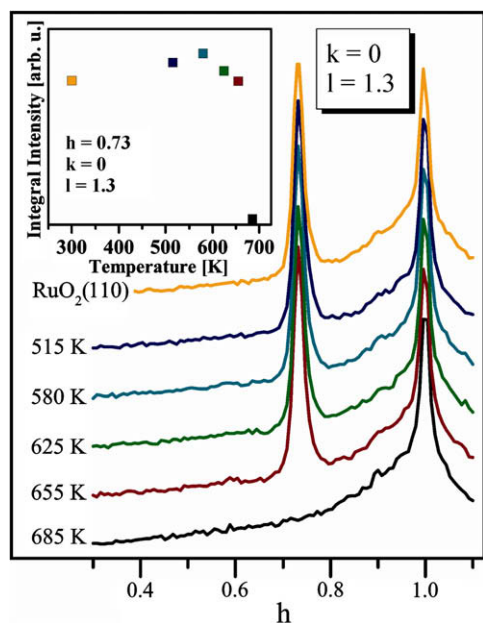


Fig. 3. Structural stability measurements of $\text{RuO}_2(1\ 1\ 0)$ under pure HCl exposure of $p(\text{HCl}) = 1$ mbar and various temperatures ranging from 300 K to 685 K. Shown are h -scans for $k = 0$ and $l = 1.3$, revealing the oxide peak at $h = 0.73$ and the surface $\text{Ru}(0\ 0\ 0\ 1)$ peak at $h = 1.0$. Below 600 K, the oxide surface is stable as indicated by the integral intensity as a function of the sample temperature (cf. inset). Chemical reduction of the $\text{RuO}_2(1\ 1\ 0)$ sets in around 655 K and is completed at 685 K.

reduction temperature is much higher, namely above 655 K. Obviously, the rate-determining step of this reduction process is distinctively different from that with H_2 and MeOH . For HCl exposure above 500 K, part of the bridging O atoms of the stoichiometric $\text{RuO}_2(1\ 1\ 0)$ surface are replaced by chlorine, and this process is selective and self-limiting. Recent density functional theory (DFT) calculations indicate that the actual chlorination process of the $\text{RuO}_2(1\ 1\ 0)$ surface is mediated by the formation of a bridging water species [24] which is produced either by H transfer from adsorbed HCl at a 1f-cus site to a neighboring $\text{O}_{\text{br}}\text{-H}$ group or by the recombination of two neighboring $\text{O}_{\text{br}}\text{-H}$ groups.

At 500 K the side-product water desorbs. Additional HCl adsorption does not lead to further incorporation of chlorine into the oxygen sublattice of $\text{RuO}_2(1\ 1\ 0)$. One reason for the observed HCl-tolerance is traced to the endothermic adsorption of HCl on the fully chlorinated $\text{RuO}_2(1\ 1\ 0)$ surface when no under coordinated surface O is available [24]. The second reason is that part of the 1f-cus Ru sites is blocked by on-top Cl which is produced during the chlorination process of the bridge site for stoichiometry reasons: In order to replace one bridging O atom, two HCl molecules have to transfer their H atom to bridging O atoms. Therefore, two chlorine atoms are formed at the surface, one shifting into the bridge position and the other stays at the 1f-cus site.

But what happens above 650 K? At these high temperatures, on-top Cl recombines to form Cl_2 , producing vacant 1f-cus sites. Subsequently, bridging chlorine is able to shift to the vacant 1f-cus sites and recombines with adjacent on-top chlorine to form molecular chlorine which is immediately released into the gas phase [14,15]. The so produced vacant bridge sites are quickly filled in by diffusion of bulk oxygen from below, a process which was proposed some years ago [25] and only recently was identified by an in situ RAIRS study [26]. Now HCl from the gas phase can readily adsorb on the vacant 1f-cus Ru sites by transferring H to the newly formed bridging O atoms forming eventually water which desorbs at temperatures above 420 K. In this way, the $\text{RuO}_2(1\ 1\ 0)$ is gradually reduced. The reduction of $\text{RuO}_2(1\ 1\ 0)$

oxide sets in only above 650 K when chlorine can desorb from the surface.

A similar reduction experiment with pure HCl exposure (1 mbar) was conducted with the $\text{RuO}_2(1\ 0\ 0)$ surface. The stability experiments in Fig. 4 indicate, however, that this surface orientation is stable up to 600 K under 1 mbar of HCl. At 615 K, the oxide disappears gradually with exposure time. The stability temperature is only slightly lower than of the $\text{RuO}_2(1\ 0\ 0)$ surface.

We surmise that again adsorbed chlorine is inhibiting the reduction process at temperatures below 600 K. As soon as chlorine can be released from the bridge position and subsequently leaves the surface by associative desorption, reduction of the $\text{RuO}_2(1\ 0\ 0)$ surface sets in.

From these stability experiments, we conclude that the RuO_2 surfaces are stable up to 600 K in the HCl oxidation reaction independent on the actual reaction mixture. In Section 3.3, where we discuss the activity experiments, we show also that both $\text{RuO}_2(1\ 1\ 0)$ and $\text{RuO}_2(1\ 0\ 0)$ are stable under a stoichiometric $\text{HCl} + \text{O}_2$ reaction mixture at 650 K. For a reaction mixture $p(\text{HCl}):p(\text{O}_2) = 1:1$, the $\text{RuO}_2(1\ 1\ 0)$ surface is even stable up to 680 K.

3.2. Stability experiments under oxidizing reaction conditions

Here, we present stability data of $\text{RuO}_2(1\ 1\ 0)$ and $\text{RuO}_2(1\ 0\ 0)$ which were exposed to a strongly oxidizing reaction mixture consisting of $p(\text{HCl}) = 1$ mbar and $p(\text{O}_2) = 4$ mbar at 685 K and 650 K, respectively.

The thickness can be followed in situ by consecutive l -scans of the oxide-related reflections. Using the Debye–Scherrer formula, the full width at half maximum (FWHM) of the peak in the l -scan can be correlated with the averaged thickness of the oxide film. In Fig. 5, the FWHM of the diffraction peaks in the corresponding l -scans at $(h, k) = (0.73, 0)$ for $\text{RuO}_2(1\ 1\ 0)$ and $(h, k) = (0.88, 0)$ for $\text{RuO}_2(1\ 0\ 0)$ are shown as a function of the exposure time. The

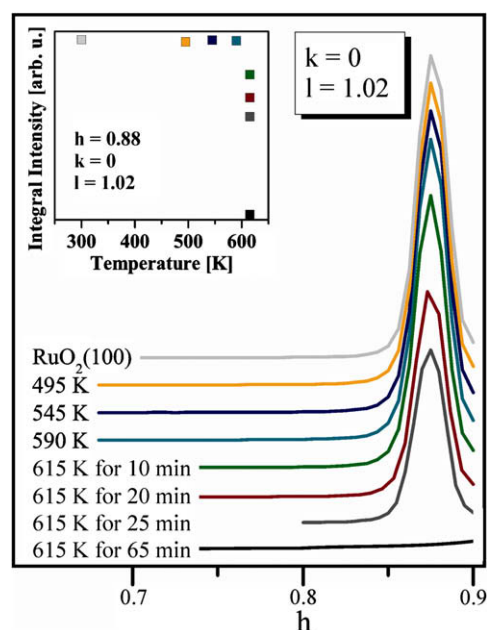


Fig. 4. Structural stability measurements of $\text{RuO}_2(1\ 0\ 0)$ under pure HCl exposure of $p(\text{HCl}) = 1$ mbar and various temperatures ranging from 495 K to 615 K. Shown are h -scans at $k = 0$ and $l = 1.02$. Below 600 K, the $\text{RuO}_2(1\ 0\ 0)$ is stable, as indicated by the invariance of the integral intensities of the $h = 0.88$ diffraction feature as a function of temperature and at 615 K as a function of time (inset). Chemical reduction of the $\text{RuO}_2(1\ 0\ 0)$ proceeds slowly at 615 K. Keeping the sample at 615 K in 1 mbar of HCl, the oxide has eventually disappeared after 65 min.

$\text{RuO}_2(1\ 0\ 0)$ exhibits a slight growth of the oxide at the beginning, where the FWHM decrease from 0.12 to 0.105 corresponding to an increase of the averaged film thickness from 4.3 nm to 4.7 nm. A similar behavior is observed with the $\text{RuO}_2(1\ 1\ 0)$ surface. During the first 2 h, the $\text{RuO}_2(1\ 1\ 0)$ film grows thicker as indicated by a decrease of the FWHM from 0.185 to 0.16 which corresponds to an averaged film thickness variation of 2.5–2.8 nm. Subsequently, the oxide growth is significantly slower. During the next 12 h, only a slight decrease of the FWHM to 0.14 is observed which corresponds to a thickness of 3.2 nm.

These experiments provide evidence that HCl in the reaction mixture does not suppress the further oxide growth, when the reaction mixture is net oxidizing, and the reaction temperature is above 650 K. This finding can be explained by the recently observed dynamical response of bridging chlorine when on-top oxygen is also present on the $\text{RuO}_2(1\ 1\ 0)$ surface [24]. On-top adsorbed oxygen replaces the bridging chlorine for energy reasons, leading to a re-oxidation of the chlorinated $\text{RuO}_2(1\ 1\ 0)$ surface. We expect that this process of re-oxidation also mediates the further oxide growth under oxidizing reaction conditions.

3.3. Activity experiments

In the following, we present structure–activity data of $\text{RuO}_2(1\ 1\ 0)$ and $\text{RuO}_2(1\ 0\ 0)$ for a stoichiometric reaction mixture $p(\text{HCl}) = 2$ mbar and $p(\text{O}_2) = 0.5$ mbar. This situation differs from the optimum reaction conditions as reported recently for RuO_2 powder catalysts [15]. However, with the chosen reaction mixture, mass spectrometry (MS) is most sensitive to changes of the partial oxygen pressures. In order to calibrate the oxygen MS signal, 1 mbar of Ar was added to the reaction mixture. The surface structure of the oxides was followed by in situ XRD during the reaction. For the case of $\text{RuO}_2(1\ 1\ 0)$ and $\text{RuO}_2(1\ 0\ 0)$, the data are presented in Figs. 6 and 7, respectively; the reaction temperature was 650 K. As can be seen from the bottom inset of Figs. 6 and 7, the oxide surfaces are stable under these reaction conditions over more than 15 h independent of the reaction temperature. The integral intensities of the oxide-related diffraction peaks in the h-scans are constant. Neither the surface areas nor the thickness of the oxide changes as determined by the invariance of the FWHM of the oxide-related peak intensities in the h- and l-scans.

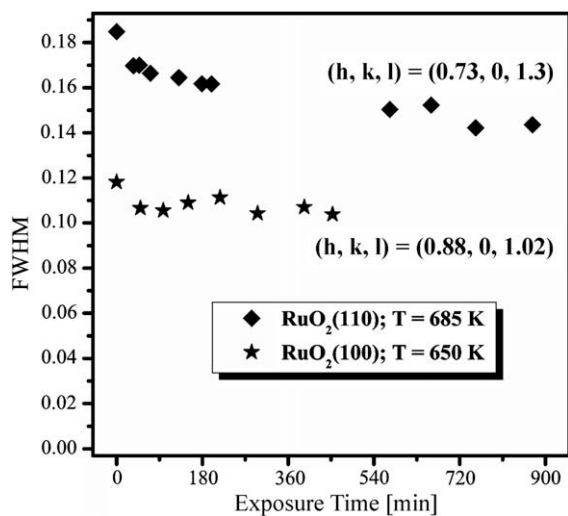


Fig. 5. Stability of $\text{RuO}_2(1\ 1\ 0)$ and $\text{RuO}_2(1\ 0\ 0)$ against oxidizing reaction conditions $p(\text{HCl}) = 1$ mbar and $p(\text{O}_2) = 4$ mbar at $T = 685$ K and 650 K, respectively. Shown are the FWHM of the oxide-related peak in the l-scans of $\text{RuO}_2(1\ 1\ 0)$ and $\text{RuO}_2(1\ 0\ 0)$ as a function of exposure time. Both oxides grow slightly in thickness over a time period of 8 h respectively 14 h.

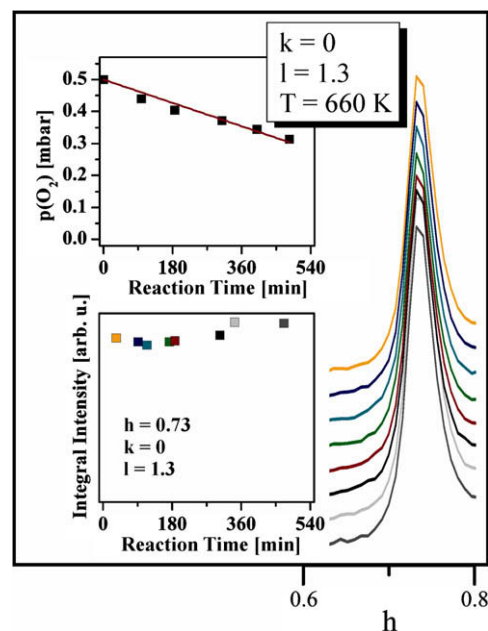


Fig. 6. Structure–activity measurements of the $\text{RuO}_2(1\ 1\ 0)$ surface under stoichiometric reaction conditions, i.e., $p(\text{HCl}) = 2$ mbar and $p(\text{O}_2) = 0.5$ mbar at $T = 650$ K. The oxide surface is stable under these reaction conditions as indicated by the h-scans around the oxide peak (for clarity consecutive h-scans are shifted vertically by a constant value) and by the constant integral intensity of the oxide-related diffraction peak at $(h, k, l) = (0.73, 0, 1.3)$ as a function of reaction time (bottom inset). The time evolution of the partial pressure of oxygen during the reaction is shown in the upper inset. From this decay, a mean TOF of 0.6 Cl_2 molecules per second and active site is derived.

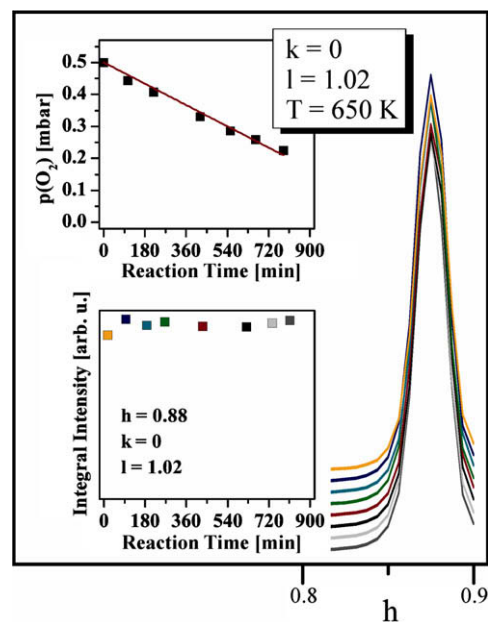


Fig. 7. Structure–activity measurements stability of the $\text{RuO}_2(1\ 0\ 0)$ surface under stoichiometric reaction conditions, i.e., $p(\text{HCl}) = 2$ mbar and $p(\text{O}_2) = 0.5$ mbar at $T = 650$ K. The oxide surface is stable under reaction conditions as indicated by the invariance of the h-scans around the oxide peak (for clarity consecutive h-scans are shifted vertically by a constant value) and by the constant integral intensity of the oxide-related diffraction peak at $(h, k, l) = (0.88, 0, 1.02)$ as a function of reaction time (bottom inset). The decline of the partial pressure of oxygen during the reaction is shown in upper inset. From this decay a mean TOF of 0.6 Cl_2 molecules per second and active site is calculated.

In Figs. 6 and 7 (upper insets), we summarize the reactivity data which were taken with on-line mass spectrometry. From the time

evolution of the O₂ partial pressure, we can derive the turn-over frequency (TOF), which is defined as the number of produced Cl₂ molecules per active site and second. The TOF is calculated from the following formula

$$\text{TOF} = -\frac{2V \cdot L}{R \cdot T} \cdot \frac{1}{\#\text{Cat}} \cdot \frac{dp(\text{O}_2)}{dt} \quad (1)$$

with V = volume of the batch reactor = 2 dm³, L = Avogadro's number = 6.022×10^{23} 1/mol, R = general gas constant = 8.314 J/(Kmol), T = gas temperature = 300 K, $\#\text{Cat}$ = number of active catalyst sites = estimated to be 10^{15} (the sample area is 1 cm²) = number of available 1f-cus Ru sites on the sample surface.

We may note that the batch reactor is not running under isothermal conditions, i.e. the gas temperature differs from the temperature of the model catalyst surface. Most of the gas molecules are close to room temperature (the temperature of the chamber walls), while the sample (model catalyst) can be heated deliberately to the desired temperature (typical 650 K). This temperature difference results in an uncertainty in the actual gas temperature T which enters Eq. (1) for the calculation of the TOF.

For both RuO₂(1 1 0) and RuO₂(1 0 0) surfaces, the mean TOF at 650 K and $p(\text{HCl}) = 2$ mbar, $p(\text{O}_2) = 0.5$ mbar turned out to be 0.6 s^{-1} and active site for a gas temperature of 300 K (and 0.28 s^{-1} for a gas temperature of 650 K just for comparison). At least for these two orientations the activity is identical so that we surmise that the HCl oxidation reaction of RuO₂ is structure insensitive. To the best of our knowledge, this is the first report of an experimental turn-over frequency of the HCl oxidation over RuO₂. This datum will serve as a benchmark for future experiments and theoretical work. A TOF value of 0.6 s^{-1} precludes mass transfer limitations during the catalyzed reaction. Using kinetic gas theory, the collision number of reactant molecules (2 mbar, $T = 300$ K) with the sample surface can be determined to be $3 \times 10^{+20}$ per second. Since the actual number of reactant molecules to be consumed by the surface reaction is only about 10^{+15} per second, the transport of reactant molecules toward the catalyst surface can be ruled out to be rate-limiting. There is also no heat transfer limitation, since the deposited heat power (due to reaction exothermicity) on the surface is as low as 8×10^{-5} W; compare the discussion in Ref. [27]. A recent theoretical study by Studt et al. [28] has estimated the TOF to be 20 s^{-1} for the HCl oxidation reaction over RuO₂(1 1 0) at $T = 573$ K and pressures of 1 bar. This value is consistent with our value, since the used reactant pressures are significantly higher (1 bar vs. 2 mbar), the stoichiometry of the gas feed was chosen to be 1:1 (O₂:HCl) instead of 1:4, and the reaction temperature was 573 K instead of 650 K.

We may discuss the relevance of kinetic data obtained for a batch reactor with those for flow reactor. First of all we should emphasize that the present reactivity experiments relied on a batch reactor, since the active surface area of our sample is only 1 cm², and the resulting TOF for the HCl oxidation reaction is quite low with 0.6 s^{-1} . The kinetic data obtained by a batch reactor can of course be compared with a flow reactor: The concentration profile of reactants and products along the catalyst bed of an industrial flow reactor is roughly mimicked by the time evolution of the batch reactor. If we determine the initial rate (instead of the mean TOF) in the batch reactor, this initial TOF value can be compared directly with a flow reactor applying a very thin catalyst bed (or alternatively, the reactivity at the very beginning of the catalyst bed), while the reactivity for very long reaction times in the batch reactor reflects the activity of the catalyst bed in the exit part. In this sense, kinetic data of a batch reactor are also useful for industrial flow type reactors and the resulting TOF value should agree within an order of magnitude.

The reaction mechanism for the HCl oxidation has been elucidated for the model catalyst RuO₂(1 1 0) and RuO₂ powder catalysts by a combined theory/experiment approach [14,15,28]. The kinetics of the HCl oxidation reaction over chlorinated RuO₂(1 1 0), where all bridging O atoms are replaced by chlorine, is purely governed by surface thermodynamics [14], i.e. the adsorption energies of the reaction intermediates (water: 109 kJ/mol and on-top Cl: 115 kJ/mol) rather than by true kinetic barriers. During the reaction, the reactive intermediates are continuously replenished. Dissociative adsorption of O₂ is non-activated, forming atomic O in atop position of the 1f-cus Ru sites. The on-top O species in turn stabilizes HCl adsorption on the chlorinated RuO₂(1 1 0) surface; recall that without the presence of under coordinated surface oxygen, HCl adsorption is endothermic and therefore suppressed. HCl adsorbs first on 1f-cus sites in close proximity to the terminal O_{ot} species to which the H atom is instantaneously transferred without any noticeable activation barrier. The final production of surface water (H₂O_{ot}) via H transfer between two neighboring O_{ot}H groups is kinetically activated by only 29 kJ/mol. The recombination of two on-top Cl species to form the desired product Cl₂ constitutes the rate-determining step with an activation barrier of 115 kJ/mol.

Poisoning of the model catalysts by re-adsorption of Cl₂ from the gas phase is not observed in the present kinetic data. The reaction order cannot be determined with confidence. However, the time evolution of the partial pressure of oxygen shown in Figs. 6 and 7 can be compared to known integral time laws for zero and first-order kinetics in oxygen. Zero-order kinetics is characterized by a linear decrease of the partial O₂ pressure with time, while first-order kinetics results in an exponential decay of the partial pressure. This comparison reveals a significantly better fit of the experimental data with first-order kinetics than with zero-order kinetics.

4. Conclusion

In situ surface X-ray diffraction (SXRD) in combination with on-line mass spectrometry was employed to explore the structure/activity correlation of the HCl oxidation catalyzed by RuO₂ model catalysts. These experiments reveal that the chlorinated RuO₂(1 1 0) and RuO₂(1 0 0) model catalysts for the Sumitomo process are long-term stable under reaction conditions where the stoichiometry of the gas feed $p(\text{HCl}):p(\text{O}_2)$ varies from 1:4 to 4:1 for pressures in mbar range and temperatures as high as 685 K. Even pure HCl exposure in the mbar range is not able to reduce the RuO₂ below 600 K since adsorbed chlorine blocks under coordinated Ru sites and without the presence of under coordinated surface oxygen, HCl adsorption is suppressed for thermodynamic reasons. Above 620 K, chemical reduction of the oxide sets in. Under strongly oxidizing reaction conditions, the oxide grows slowly in thickness. Reactivity experiments in a batch reactor indicate a mean turn-over frequency of 0.6 Cl_2 molecules per second and active site for the HCl oxidation at 650 K and partial pressures $p(\text{HCl}) = 2$ mbar and $p(\text{O}_2) = 0.5$ mbar independent of the model catalyst – RuO₂(1 1 0) and RuO₂(1 0 0) – suggesting the HCl-oxidation over RuO₂ to be structure insensitive. These findings will serve as a benchmark for future more elaborated experimental and theoretical studies. Concomitant in situ SXRD experiments show that both model catalysts are stable under stoichiometric reaction conditions.

Acknowledgments

S.Z., H.O. thank the German Research Council and J.P.H., H.O. the Federal Ministry for Science and Education (BMBF_Deacon:

033R018C) for financial support. E.L. acknowledges the Swedish Research Council for financial support. We would like to thank the ESRF_ID03 staff for technical support.

References

- [1] H. Deacon, US Patent (1875) 0165802.
- [2] J.A. Allen, A.J. Clark, *Rev. Pure Appl. Chem.* 21 (1971) 145.
- [3] F. Wattimena, W.M.H. Sachtler, *Stud. Surf. Sci. Catal.* 7 (1981) 816.
- [4] J.T. Quant, J. van Dam, F. Engel, F. Wattimena, *Chem. Eng. July/August* (1963) 224.
- [5] Mitsui Toatsu chemicals: a modern version of the Deacon process. *Chem. Week* 18 (1987) (June 24).
- [6] M. Mortensen, R.G. Minet, T.T. Tsotsis, S. Benson, *Chem. Eng. Sci.* 15 (1996) 2031.
- [7] U. Nieken, O. Watzenberger, *Chem. Eng. Sci.* 54 (1999) 2619.
- [8] F. Gestermann, A. Ottavini, *Mod. Chlor. Alkali Technol.* 8 (2001) 49–56.
- [9] K. Iwanaga, K. Seki, T. Hibi, K. Isoh, T. Suzuta, M. Nakada, Y. Mori, T. Abe, The development of improved hydrogen chloride oxidation process, Sumitomo Kagaku I (2004) 1–11.
- [10] S. Trassati, in: A. Wieckowski (Ed.), *Interfacial Electrochemistry*, Marcel Dekker Inc., Basel, 1999, pp. 769–792 (and references therein).
- [11] V.R. Stamenkovic, B. Fowler, B.S. Mun, G. Wang, P.N. Ross, C.A. Lucas, N.M. Markovic, *Science* 315 (2007) 493.
- [12] J.K. Nørskov, T. Bligaard, J. Rossmeisl, C.H. Christensen, *Nat. Chem.* 1 (2009) 37.
- [13] D. Crihan, M. Knapp, S. Zweidinger, E. Lundgren, C.J. Weststrate, J.N. Andersen, A.P. Seitsonen, H. Over, *Angew. Chem. Int. Ed.* 47 (2008) 2131.
- [14] S. Zweidinger, D. Crihan, M. Knapp, J.P. Hofmann, A.P. Seitsonen, C.J. Weststrate, E. Lundgren, J.N. Andersen, H. Over, *J. Phys. Chem. C* 112 (2008) 9966.
- [15] N. López, J. Gómez-Segura, R.P. Marín, J. Pérez-Ramírez, *J. Catal.* 255 (2008) 29.
- [16] G. Ertl, *Angew. Chem. Int. Ed.* 29 (1990) 1219.
- [17] O. Balmes, R. van Rijn, D. Wermeille, A. Resta, L. Petit, H. Isern, T. Dufrane, R. Felici, *Catal. Today* 145 (2009) 220–226.
- [18] P. Bernhard, K. Peters, J. Alvarez, S. Ferrer, *Rev. Sci. Instrum.* 70 (1999) 1478.
- [19] Y.B. He, M. Knapp, E. Lundgren, H. Over, *J. Phys. Chem. B* 109 (2005) 21825.
- [20] M. Knapp, A.P. Seitsonen, Y.D. Kim, H. Over, *J. Phys. Chem. B* 108 (2004) 14392.
- [21] H. Over, Y.D. Kim, A.P. Seitsonen, S. Wendt, E. Lundgren, M. Schmid, P. Varga, A. Morgante, G. Ertl, *Science* 287 (2000) 1474–1476.
- [22] M. Knapp, D. Crihan, A.P. Seitsonen, E. Lundgren, A. Resta, J.N. Andersen, H. Over, *J. Phys. Chem. C* 111 (2007) 5363–5373.
- [23] R. Blume, M. Hävecker, S. Zafeirotos, D. Teschner, A. Knop-Gericke, R. Schlögl, S. Lizzit, P. Dudin, A. Barinov, M. Kiskinova, *Phys. Chem. Chem. Phys.* 6 (2007) 3648.
- [24] J.P. Hofmann, PhD thesis, JLU Giessen, 2009. <<http://geb.uni-giessen.de/geb/volltexte/2010/7411/>>.
- [25] S. Wendt, A.P. Seitsonen, Y.D. Kim, M. Knapp, H. Idriss, H. Over, *Surf. Sci.* 505 (2002) 137.
- [26] A. Farkas, G. Mellau, H. Over, *J. Phys. Chem. C* 113 (2009) 14341.
- [27] H. Over, O. Balmes, E. Lundgren, *Surf. Sci.* 603 (2009) 298.
- [28] F. Studt, F. Abild-Pedersen, H.A. Hansen, I.C. Man, J. Rossmeisl, T. Bligaard, *Chem. Cat. Chem.* 2 (2010) 98.